Article

Cell Reports

IDH1 Mutation Promotes Tumorigenesis by Inhibiting JNK Activation and Apoptosis Induced by Serum Starvation

Graphical Abstract

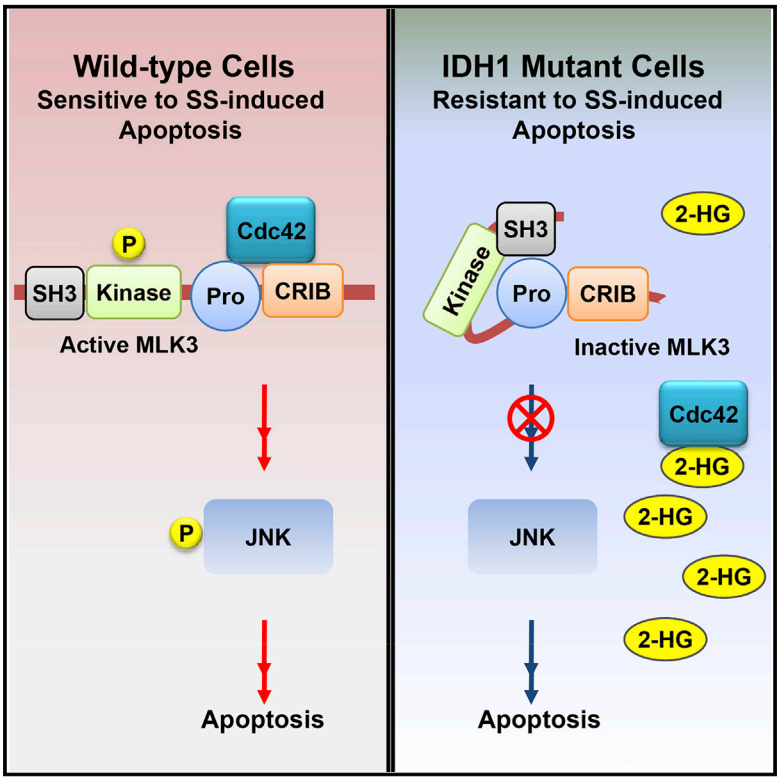

Highlights

- JNK activation is a key event in apoptosis triggered by SS
- 2-HG profoundly inhibits JNK activation induced by SS
- 2-HG physically binds to Cdc42 and abolishes its association with MLK3
- Loss of JNK-mediated apoptosis is a key event in tumorigenesis driven by 2-HG

Authors

Bin Jiang, Jia Zhang, Jinmei Xia, ..., Li-Man Hung, Tak Wah Mak, Qinxi Li

Correspondence

liqinxi@xmu.edu.cn

In Brief

Jiang et al. report that oncometabolite 2-HG, produced by tumor-associated IDH1 mutation, physically binds to Cdc42 and abolishes its association with MLK3 and consequently disrupts JNK activation and apoptosis induced by serum deprivation. Loss of JNK-mediated apoptosis may be a key event in tumorigenesis driven by 2-HG.

Jiang et al., 2017, Cell Reports *19*, 389–400
April 11, 2017
http://dx.doi.org/10.1016/j.celrep.2017.03.053

Cell Reports
Article

IDH1 Mutation Promotes Tumorigenesis by Inhibiting JNK Activation and Apoptosis Induced by Serum Starvation

Bin Jiang,[1,8] Jia Zhang,[1,8] Jinmei Xia,[2,8] Wentao Zhao,[1] Yanan Wu,[1] Minggang Shi,[3] Lianzhong Luo,[4] Huamin Zhou,[1] Ai Chen,[1] Huanhuan Ma,[1] Qingwen Zhao,[1] Muhammad Suleman,[1] Furong Lin,[1] Lin Zhou,[1] Jinyang Wang,[1] Yan Zhang,[1] Ying He,[1] Xiaotong Li,[1] Li-Man Hung,[5,6] Tak Wah Mak,[7] and Qinxi Li[1,7,9,*]

[1]State Key Laboratory of Cellular Stress Biology, Innovation Center for Cell Signaling Network, School of Life Sciences, Xiamen University, Xiamen, Fujian 361102, China
[2]Key Laboratory of Marine Biogenetic Resources, Third Institute of Oceanography, State Oceanic Administration, Xiamen 361005, China
[3]Department of Neurosurgery, Huanhu Hospital, No. 6 Jizhao Road, Jinnan District, Tianjin, 30050, China
[4]Xiamen Key Laboratory of Marine Medicinal Natural Products and Cell Engineering, Xiamen Medical College, Xiamen 361008, China
[5]Department and Graduate Institute of Biomedical Sciences, College of Medicine, Chang Gung University, Tao-Yuan 33302, Taiwan
[6]Department of Anesthesiology, Chang Gung Memorial Hospital, Tao-Yuan 33302, Taiwan
[7]The Campbell Family Institute for Breast Cancer Research, Ontario Cancer Institute, University Health Network, Toronto, ON M5G 2C1, Canada
[8]Co-first author
[9]Lead Contact
*Correspondence: liqinxi@xmu.edu.cn
http://dx.doi.org/10.1016/j.celrep.2017.03.053

SUMMARY

Two hallmarks of cancer cells are their resistance to apoptosis and ability to thrive despite reduced levels of vital serum components. c-*jun* N-terminal kinase (JNK) activation is crucial for apoptosis triggered by serum starvation (SS), and isocitrate dehydrogenase 1 (IDH1) mutations are tumorigenic, in part, because they produce the abnormal metabolite 2-hydroxyglutarate (2-HG). However, it is unknown whether 2-HG-induced tumorigenesis is partially due to JNK inhibition and thus defective SS-induced apoptosis. We show here, using IDH1-R132Q knockin mutant mouse cells, that 2-HG inhibits JNK activation induced only by SS and not by UV or doxorubicin, and thus can block apoptosis. Upon SS, Cdc42 normally disrupts mixed lineage kinase 3's (MLK3's) auto-inhibition, triggering the MLK3-MKK4/7-JNK-Bim apoptotic cascade. 2-HG binds to Cdc42 and abolishes its association with MLK3, inactivating MLK3 and apoptosis. Allograft tumor assays in mice demonstrate that this mechanism contributes to tumorigenesis driven by mutant IDH1, a result confirmed by detection of JNK inactivation in human gliomas harboring IDH1-R132H mutations.

INTRODUCTION

Isocitrate dehydrogenases (IDHs) normally convert isocitrate to α-ketoglutarate (α-KG) in a $NAD(P)^+$-dependent manner. Three IDH isozymes that operate in distinct subcellular compartments exist: IDH1, IDH2, and IDH3. In the past few years, various somatic point mutations of *IDH1* or *IDH2* have been identified in a broad range of cancers, including glioma (Hirata et al., 2015; Parsons et al., 2008; Yan et al., 2009), sarcoma (Amary et al., 2011), and acute myeloid leukemia (AML) (Mardis et al., 2009), among others. These mutations, which include IDH1 R132H/C/Q, IDH2 R140Q/W/L, and R172K/M/G/T/S, all confer a novel catalytic activity on the mutant IDH protein that converts α-KG to the oncometabolite 2-hydroxyglutarate (2-HG) (Dang et al., 2009; Ward et al., 2010). In human glioma samples harboring IDH1/2 mutations, 2-HG can accumulate to the astonishingly high level of 5–35 μmol/g, which is ~100-fold greater than its level in a normal brain (Dang et al., 2009).

Due to its structural similarity to α-KG, 2-HG functions as a competitive inhibitor of α-KG-dependent dioxygenases (Xu et al., 2011). Accordingly, elevated levels of 2-HG inhibit TET2, an α-KG-dependent dioxygenase that catalyzes the conversion of 5-methylcytosine (5mC) to 5-hydroxylmethylcytosine (5hmC), which is a prerequisite for DNA demethylation (Xu et al., 2011). Several lines of evidence indicate that the excessive 2-HG production mediated by mutated IDH1 results in DNA hypermethylation (Noushmehr et al., 2010). In addition to its effects on TET2, 2-HG blocks α-KG-dependent histone demethylases, which disrupts cell differentiation (Lu et al., 2012). Furthermore, 2-HG increases murine hematopoietic progenitors in IDH1 R132Q-expressing mice (Sasaki et al., 2012b) and perturbs collagen maturation by inhibiting α-KG-dependent dioxygenases involved in this process (Sasaki et al., 2012a). With respect to cancer, several groups have reported that 2-HG may stimulate tumorigenesis by inhibiting hypoxia-inducible factor (HIF) prolyl hydroxylase (PHD), which stabilizes HIF-1α (Xu et al., 2011; Zhao et al., 2009). However, other groups have shown that

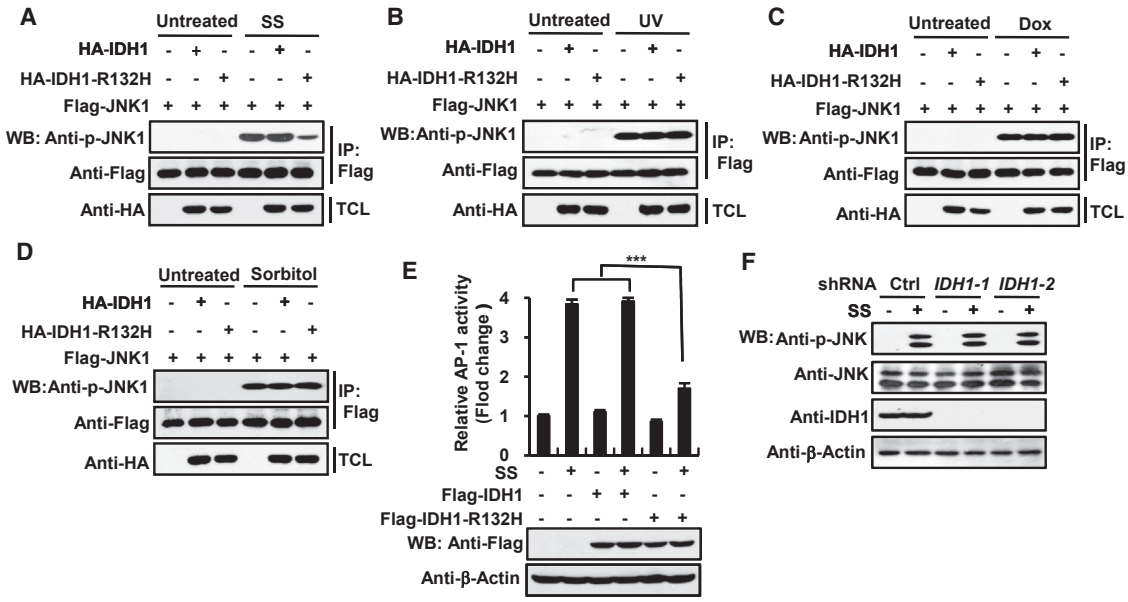

Figure 1. IDH1-R132H Inhibits JNK Phosphorylation Induced Only by SS

(A–D) HEK293T cells were transfected with the indicated plasmids, and 24 hr later, were left untreated (–) or subjected to (+) (A) SS for 9 hr, (B) UV (80 J/m^2) followed by culture for 4 hr, (C) 2.5 μM Dox for 8 hr, or (D) 0.1 M sorbitol for 4 hr. Top: total cell lysates (TCLs) were subjected to immunoprecipitation (IP) with anti-Flag M2 beads to isolate Flag-JNK1, and phospho-JNK and Flag-JNK were detected by WB. Bottom: WB of TCL of cells in the top panel to detect HA-IDH1 and HA-IDH1-R132H.

(E) HEK293T cells were co-transfected with AP-1 firefly luciferase reporter plus renilla luciferase vector (as an internal control), together with empty vector or vector expressing Flag-IDH1 or Flag-IDH1-R132H. Cells were left untreated (–) or subjected to SS (+) for 9 hr. Top: quantitation of firefly luciferase activity following normalization to renilla luciferase activity. Results are the mean ± SD of three independent experiments (***$p < 0.001$, unpaired Student's t test). Bottom: WB to detect IDH proteins in the cells in the top panel. β-actin, loading control.

(F) WB to detect the indicated proteins in HEK293T cells that were transfected with control shRNA (Ctrl) or one of two different shRNAs against *IDH1* (*IDH1-1*, *IDH1-2*) and were left untreated or subjected to SS for 9 hr.

2-HG can downregulate HIF-1α, a function that may stimulate tumorigenesis in situations in which HIF-1α functions as a tumor suppressor (Koivunen et al., 2012). Taken together, these data establish that 2-HG-mediated inhibition of various hydroxylation reactions plays an important role in the tumorigenesis driven by IDH1/2 mutations.

It is now clear that programmed cell death serves as a natural barrier to cancer initiation and development. Because of their uncontrolled proliferation, cancer cells often find themselves in a microenvironment characterized by hypoxia and a minimal supply of serum components. Such severe serum starvation (SS) eventually induces the apoptosis of these tumor cells, restricting the expansion of the growing cell mass (Izuishi et al., 2000; Ou et al., 2006). It has long been known that activation of the c-*jun* N-terminal kinase (JNK) signaling cascade is involved in neuronal cell apoptosis induced by nerve growth factor deprivation (Xu et al., 2001). This observation prompted us to investigate whether part of the oncogenicity of the 2-HG produced by mutant IDH enzymes was due to the effects of this abnormal metabolite on tumor cell apoptosis. In particular, we determined whether IDH1 mutation blocked the tumor cell apoptosis that would normally be mediated by JNK activation under SS conditions. Using murine IDH1-R132Q knockin mutant cells, we show that SS-induced JNK activation and apoptosis are markedly reduced by 2-HG. Mechanistically, 2-HG binds to Cdc42 and blocks its interaction with mixed lineage kinase 3 (MLK3), a kinase acting upstream of MKK4/7. This inhibition consequently switches off the MLK3-MKK4/7-JNK-Bim apoptotic cascade that is triggered by SS.

RESULTS

IDH1-R132H Mutation Robustly Inhibits SS-Induced JNK Activation

Human brain tumors frequently bear loss-of-function mutations of the *MAPK10* gene encoding JNK3 kinase, indicating that JNK may serve as a tumor suppressor in the brain (Yoshida et al., 2001). To determine whether mutant IDH1 enzymes have an inhibitory effect on JNK, we co-expressed JNK1 with wild-type (WT) IDH1 or its R132H mutant in HEK293T cells and monitored JNK phosphorylation as an indicator of JNK activity. Compared to WT IDH1, IDH1-R132H strongly repressed JNK activation induced by SS, but not that triggered by treatment with UV, doxorubicin (Dox), or sorbitol (Figures 1A–1D). In line with this result, the SS-triggered induction of the transcriptional activity of activated protein-1 (AP-1) (as evaluated by an AP-1 luciferase reporter system) was also dramatically inhibited by IDH1-R132H expression (Figure 1E). We then performed co-immunoprecipitation assays to determine whether the inhibitory effect of IDH1-R132H on JNK was due to a physical interaction

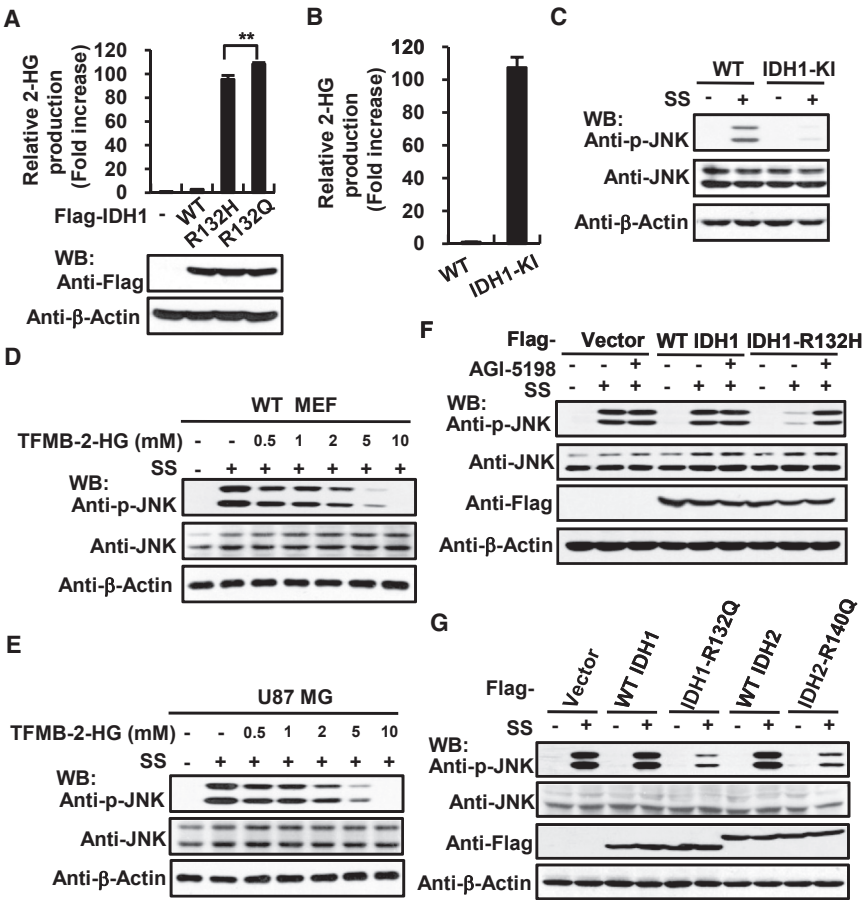

Figure 2. JNK Inhibition Induced by IDH1-R132H/Q Depends on 2-HG Production

(A) HEK293T cells were transfected with empty vector or vector expressing Flag-WT IDH1, IDH1-R132H, or IDH1-R132Q. Top: quantitation by LC-MS of 2-HG levels relative to those in cells expressing empty vector. Data are the mean ± SD of three independent experiments (**$p < 0.01$, unpaired Student's t test). Bottom: WB to detect the indicated proteins in the cells in the top panel.

(B) LC-MS quantitation of relative 2-HG production by the IDH1-WT MEF cell line and the IDH1-KI MEF cell line. Data are expressed relative to the WT level and the mean ± SD of three independent experiments.

(C) WB to detect the indicated proteins in IDH1 WT and IDH1-KI MEFs that were treated (+) or not (–) with SS for 9 hr.

(D and E) WB to detect the indicated proteins in (D) WT MEF or (E) U87 MG cells that were subjected (+) or not (–) to SS for 9 hr and treated with the indicated concentrations of TFMB-2-HG.

(F) WB to detect the indicated proteins in U87 MG cells that were transfected with empty vector or vector expressing Flag-human WT IDH1 or IDH1-R132H and were pretreated (or not) with 1.5 μM AGI-5198 for 2 days, followed by serum deprivation (or not) for another 9 hr in the presence of AGI-5198, as indicated.

(G) WB to detect the indicated proteins in U87 MG cells that were transfected with empty vector or vector expressing the indicated Flag-IDH enzymes and subjected (+) or not (–) to SS for 9 hr.

between them. However, neither WT nor mutated IDH1 was detected in the immunoprecipitates of Flag-JNK and vice versa (Figures S1A and S1B). These data demonstrate that the inhibition of SS-induced JNK activation mediated by mutated IDH1 is not due to any physical interaction between them.

It has been noted that the tumor-associated IDH1 mutant enzyme dominantly inhibits the activity of WT IDH1 by forming heterodimers (Zhao et al., 2009). To assess the possibility that IDH1-R132H might suppress SS-induced JNK activation through a dominant-negative effect on WT IDH1, we knocked down WT IDH1 expression in HEK293T cells using two different small hairpin RNAs (shRNAs) and examined JNK activation. However, loss of WT IDH1 had no discernible regulatory effect on SS-induced JNK activation (Figure 1F). Thus, the IDH1-R132H mutant enzyme's inhibitory effects on JNK activation are not due to a reduction in WT IDH1 activity.

JNK Inhibition Depends on 2-HG Production Caused by IDH1-R132H/Q Mutation

The IDH1-R132H mutation is the most frequent alteration in human glioma and leads to extremely high levels of 2-HG. The IDH1-R132Q mutation was initially observed in human chondrosarcoma and has been proven to exert the same enzymatic activity and biological functions as IDH1-R132H (Hirata et al., 2015; Inoue et al., 2016; Sasaki et al., 2012a, 2012b). To compare 2-HG levels produced by these two mutant enzymes, we overexpressed IDH1-R132H or IDH1-R132Q in HEK293T cells and measured 2-HG levels using liquid chromatography-spectrometry (LC-MS) (Dang et al., 2009). Intriguingly, cells expressing IDH1-R132Q produced more 2-HG than did IDH1-R132H-expressing cells (Figure 2A). This result prompted us to utilize the IDH1-R132Q-LSL mouse (Inoue et al., 2016; Sasaki et al., 2012a, 2012b) to investigate the inhibitory effect of mutant IDH1 on JNK activation. $IDH1^{WT/WT}$ and $IDH1^{WT/LSL}$ MEF were isolated from littermate embryos and infected with adenovirus-expressing Cre recombinase to generate an IDH1 WT cell line and an IDH1-R132Q knockin (KI) cell line, respectively. The genotypes and IDH1 protein levels of these cell lines were validated by PCR and western blotting (WB) (Figures S2A and S2B). It is important to note that our IDH1-R132Q KI MEF line was heterozygous and not homozygous for the mutation (i.e., $IDH1^{WT/R132Q}$; designated hereafter as IDH1-KI MEF). This line was deemed suitable for experiments because all somatic gain-of-function mutations of IDH1 in human malignancies have been identified exclusively in one allele (Figueroa et al., 2010). Just as observed in our IDH1-R132Q-expressing HEK293T cells, IDH1-KI MEF produced very high levels of 2-HG (Figure 2B) and exhibited dramatic suppression of SS-induced JNK activation (Figure 2C).

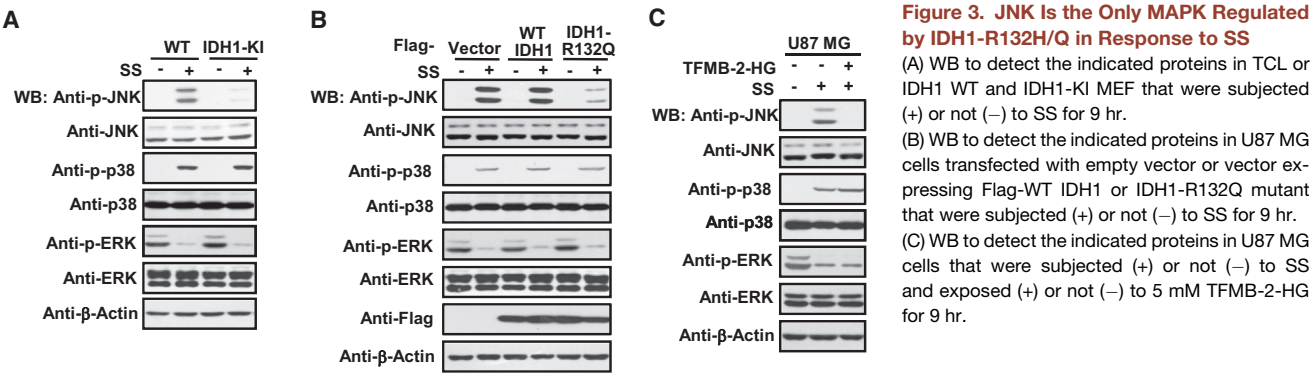

Figure 3. JNK Is the Only MAPK Regulated by IDH1-R132H/Q in Response to SS

(A) WB to detect the indicated proteins in TCL or IDH1 WT and IDH1-KI MEF that were subjected (+) or not (–) to SS for 9 hr.

(B) WB to detect the indicated proteins in U87 MG cells transfected with empty vector or vector expressing Flag-WT IDH1 or IDH1-R132Q mutant that were subjected (+) or not (–) to SS for 9 hr.

(C) WB to detect the indicated proteins in U87 MG cells that were subjected (+) or not (–) to SS and exposed (+) or not (–) to 5 mM TFMB-2-HG for 9 hr.

These data indicate that 2-HG may play a key role in the JNK inhibition exerted by the IDH1-R132Q mutation.

To confirm the above result, we treated WT MEF with increasing amounts of permeable trifluoromethyl benzyl-(*R*)-2-HG (TFMB-2-HG) and examined JNK activation. As shown in Figure 2D, SS-induced JNK activation was inhibited by TFMB-2-HG in a dose-dependent manner. Similar results were obtained using the U87 MG human glioma cell line, which expresses WT IDH1 (Figure 2E). In addition, we transfected U87 MG cells with vectors expressing WT IDH1 or IDH1-R132H and treated these cells with AGI-5198, a powerful and selective inhibitor of 2-HG production driven by IDH1-R132H (Rohle et al., 2013). Indeed, AGI-5198 treatment of IDH1-R132H overexpressing U87 MG cells efficiently suppressed 2-HG production (Figure S2C) and restored SS-induced JNK activation (Figure 2F). To further bolster this conclusion, we created a construct expressing IDH2-R140Q, an IDH2 mutant enzyme that also produces high levels of 2-HG (Ward et al., 2010). We transfected U87 MG cells with vectors expressing WT IDH2 or IDH1-R140Q and confirmed equivalent levels of 2-HG production as overexpression of IDH1-R132Q (Figure S2D). We then determined the effects of IDH1-R140Q overexpression on JNK activation and observed inhibition of SS-induced JNK phosphorylation to the same extent as that imposed by IDH1-R132Q overexpression (Figure 2G). Taken together, these data indicate that IDH1/2 mutant enzymes block SS-induced JNK activation because of their excessive 2-HG production.

Only SS-Induced Activation of JNK Is Regulated by IDH1-R132H/Q Mutant Enzymes

Because SS affects the activity of not only JNK but also two other MAPKs, p38 and ERK, we examined whether IDH1-R132H/Q mutations influenced SS-induced alterations to the activities of these two MAPKs. We found that SS induced the same levels of p38 activation and ERK inhibition in both IDH1 WT and IDH1-KI MEF (Figure 3A), indicating that the changes to p38 and ERK activities triggered by SS are not influenced by IDH1-R132Q. Similarly, although overexpression of IDH1-R132Q in U87 MG cells had effectively suppressed SS-induced JNK activation, it failed to alter SS-induced p38 activation or ERK inhibition (Figure 3B). Finally, although treatment of U87 MG cells with exogenous TFMB-2-HG had markedly inhibited SS-triggered JNK activation, there were not any noticeable regulatory effects on the activities of p38 and ERK (Figure 3C). These results demonstrate that under SS conditions and among the three canonical MAPKs, only JNK is regulated by the 2-HG produced by IDH1-R132H/Q.

2-HG Abrogates MLK3/MKK4/JNK Cascade Activation in Response to SS

To elucidate the mechanisms underlying the inhibitory effects of 2-HG on JNK activation, we investigated the activation of signaling cascades acting upstream of JNK. In response to stress stimuli, such as proinflammatory cytokines, UV, osmotic shock, and SS, JNK is activated by two upstream MAP kinases: MKK4 and MKK7 (Garrington and Johnson, 1999). When we examined whether MKK4/7 activation was influenced by 2-HG, we found that SS-induced MKK4/7 phosphorylation was abolished in WT MEF (Figure 4A) and U87 MG cells (Figure S3A) treated with TFMB-2-HG. IDH1-KI MEF showed complete suppression of MKK4/7 phosphorylation, regardless of TFMB-2-HG treatment (Figure 4A). Total MKK4/7 protein levels were unchanged in all cases. These data suggest that 2-HG's effects on SS-induced JNK are due to suppression of MKK4/7 activation.

SS-induced MKK4/7 phosphorylation is currently believed to be mediated by members of the MLK family, which includes MLK1–4 (Harris et al., 2002; Liu et al., 2000; Xu et al., 2001). To determine how 2-HG suppresses MKK4/7 activation, we investigated if 2-HG could downregulate the total protein levels of any MLK family members. As shown in Figure 4A, the total protein levels of MLK1–4 were comparable between WT MEF and IDH1-KI MEF and were not decreased by treatment with TFMB-2-HG. Thus, 2-HG-exerted inhibition of SS-induced MKK4/7 activation does not occur through downregulation of MLK family proteins. We next used shRNA knockdown to test the contribution of each MLK member to SS-stimulated activation of MKK4/7 and JNK. Interestingly, only shRNA-mediated interference with *MLK3* expression prevented the activation of MKK4/7 as well as JNK, demonstrating that MLK3, and not MLK1, 2, or 4, is involved in SS-induced activation of JNK signaling (Figure 4B). This observation was confirmed by a knockdown experiment performed using a different shRNA against *MLK3* (Figure S3B). Because no difference was observed in MLK3 protein levels between WT and IDH1-KI MEF, we performed in vitro kinase assays to determine whether MLK3 activity was directly inhibited by 2-HG. We overexpressed

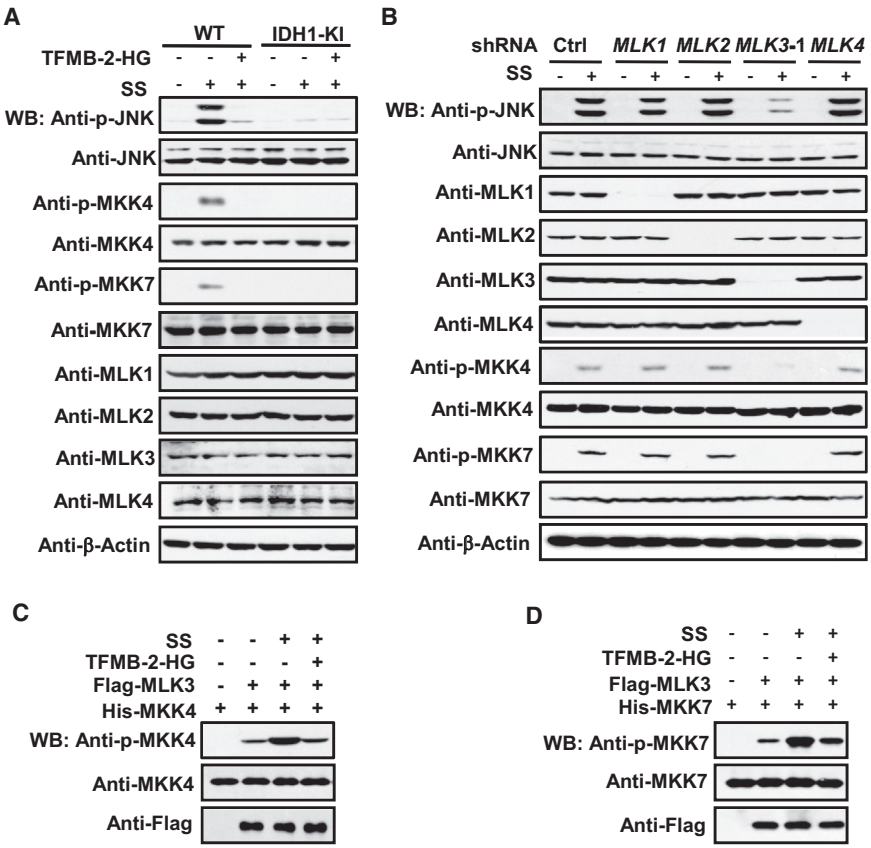

Figure 4. Mutated IDH1 Inactivates the MLK3-MKK4/7-JNK Cascade in Response to SS

(A) WB to detect the indicated proteins in IDH1 WT and IDH1-KI MEF that were subjected (+) or not (–) to SS and exposed (+) or not (–) to 5 mM TFMB-2-HG for 9 hr.

(B) WB to detect the indicated proteins in U87 MG cells that expressed control (Ctrl) shRNA or shRNA against the indicated MLK family members and were subjected (+) or not (–) to SS for 9 hr.

(C and D) MKK4/7 DKO MEF transfected with vector expressing Flag-MLK3 were treated with the indicated combinations of SS and 5 mM TFMB-2-HG for 9 hr. Flag-MLK3 was immunoprecipitated from TCL of these cells and incubated in an in vitro kinase assay with His-tagged recombinant MKK4 (C) or His-MKK7 (D) for 30 min at 37°C before WB to detect the indicated proteins.

Flag-MLK3 in double knockout (DKO) MEF lacking both *MKK4* and *MKK7* and treated these cells with various combinations of SS and TFMB-2-HG. We then incubated the immunoprecipitated Flag-MLK3 with bacterial recombinant MKK4 or MKK7 proteins in vitro and evaluated their phosphorylation status. SS treatment significantly stimulated the kinase activity of MLK3 toward MKK4 and MKK7, as indicated by increased phosphorylation, whereas the addition of 2-HG treatment completely abrogated this effect (Figures 4C and 4D). These data demonstrate that 2-HG-mediated inhibition of SS-induced JNK activation is due to its suppression of MLK3 activity.

2-HG Disrupts the Interaction between MLK3 and Cdc42

Previous studies have shown that the Rho family GTPases Cdc42 and Rac1 can both bind to MLK3 and consequently activate the MLK3-MKK4/7-JNK cascade (Coso et al., 1995; Minden et al., 1995; Teramoto et al., 1996). This binding of GTPases to MLK3 is facilitated by the presence of a Cdc42/Rac1-binding (CRIB) motif in MLK3 (Böck et al., 2000; Burbelo et al., 1995; Teramoto et al., 1996). To verify the contribution of CRIB motif to the interaction between MLK3 and Cdc42/Rac1, we examined the in vitro binding of Cdc42/Rac1 to MLK3ΔCRIB, a mutant MLK3 protein lacking the CRIB motif, and found that MLK3ΔCRIB failed to interact with Cdc42/Rac1 (Figure 5A). In addition, in contrast to WT MLK3, this deletion mutant was not activated by SS and was not suppressed by 2-HG, as revealed by in vitro kinase assays using MKK4 or MKK7 as the substrate (Figures 5B and 5C). These results demonstrate that the interaction of the CRIB motif in MLK3 with Cdc42/Rac1 is essential for SS-induced MLK3 activation as well as for 2-HG-mediated MLK3 inhibition.

We next examined precisely how 2-HG regulates MLK3 activity. An important clue from a previous study was that MLK3 activity is auto-inhibited when its SH3 domain and a region close to the CRIB motif form an intramolecular interaction (Böck et al., 2000; Zhang and Gallo, 2001). We speculated that Cdc42/Rac1 might activate MLK3 by binding to MLK3 and disrupting its autoinhibition and that 2-HG might block MLK3 activation by disrupting its interaction with Cdc42/Rac1. To test this hypothesis, we performed a series of co-immunoprecipitation assays. As expected, SS dramatically induced the interaction of MLK3 with Cdc42, and this effect was abolished by 2-HG (Figure 5D). This result was further confirmed by in vitro GST pull down assay showing that the Cdc42-MLK3 immune complex was dissociated by 2-HG in a dose-dependent manner (Figure 5E). Surprisingly, however, 2-HG failed to disrupt the interaction between MLK3 and Rac1 induced by SS (Figure 5F). These results imply that Cdc42, rather than Rac1, is involved in 2-HG-mediated inhibition of SS-induced MLK3 activity. To confirm this result, we created one MLK3 protein with the point mutation Y53A in the SH3 domain, and a second MLK3 protein with the point mutation P470A in the SH3-interacting region close to the CRIB motif. Previous investigations have shown that these specific mutations can disrupt MLK3's capacity for intramolecular interaction (Zhang and Gallo, 2001). Consistent with these observations, both of our mutant MLK3 proteins showed constitutive kinase activity toward MKK7 and were impervious to regulation by either SS or 2-HG (Figure 5G). Nevertheless, the ability of these mutant MLK3 proteins to associate with Cdc42 in response to

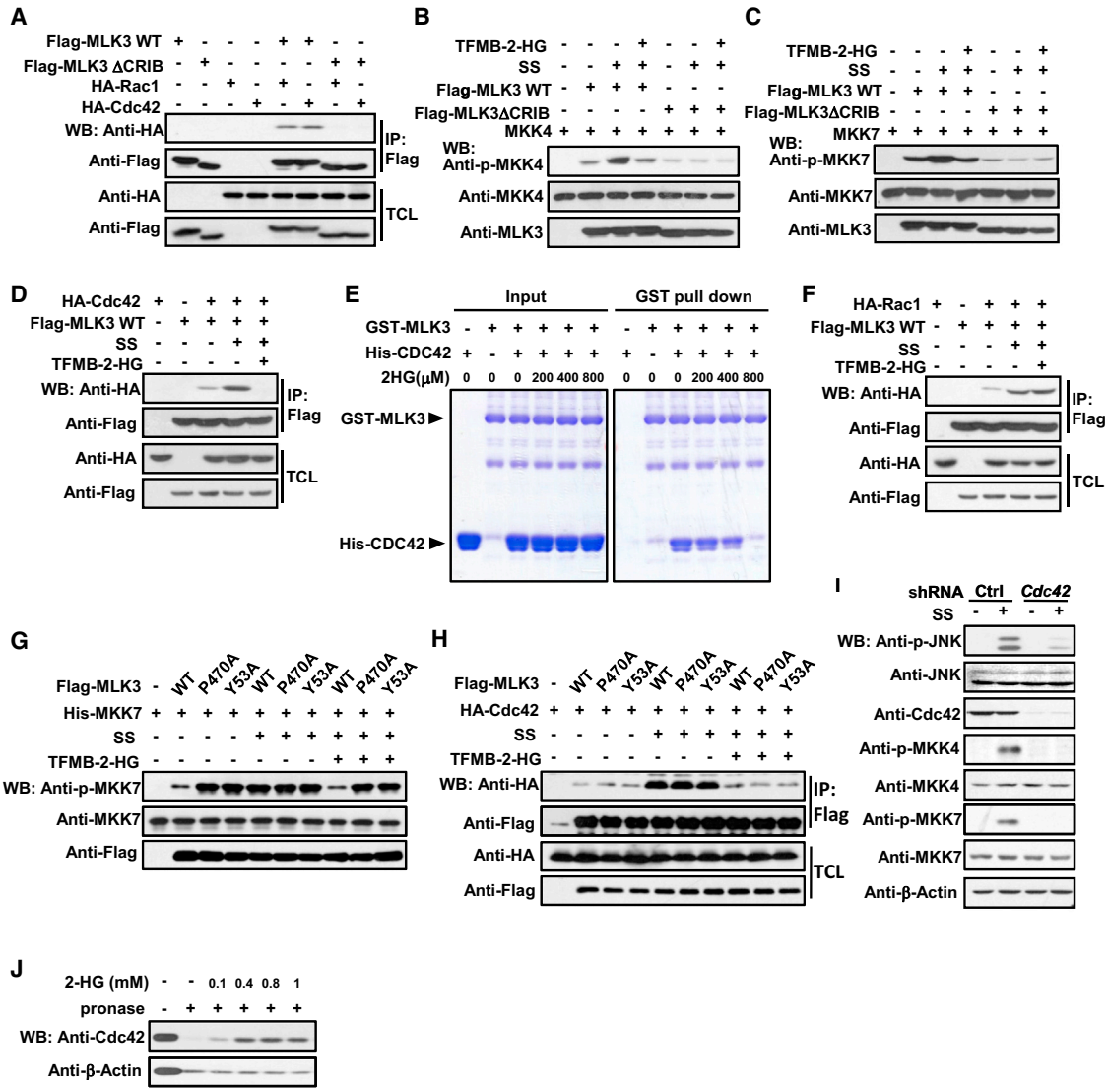

Figure 5. 2-HG Disrupts the Interaction between MLK3 and Cdc42

(A) WB to detect the indicated proteins in HEK293T cells that were transfected with the indicated combinations of vectors, followed by IP, as indicated.

(B and C) MKK4/7 DKO MEF expressing MLK3 or MLK3ΔCRIB were treated with SS alone or in combination with 5 mM TFMB-2-HG, as indicated, for 9 hr. Flag-tagged MLK3 and MLK3ΔCRIB were immunoprecipitated from TCL of these cells and incubated in an in vitro kinase assay with recombinant MKK4 (B) or MKK7 (C) for 30 min at 37°C before WB to detect the indicated proteins.

(D and F) HEK293T cells transfected with vectors expressing Flag-MLK3 plus (D) HA-Cdc42 or (F) HA-Rac1 were treated with SS and 5 mM TFMB-2-HG as in (B). IP and WB were performed to detect the indicated proteins.

(E) *E. coli* expressed His-Cdc42 and GST-MLK3 were incubated with indicated doses of 2-HG for 3 hr at 4°C. GST pull-down, SDS-PAGE, and Coomassie brilliant blue staining were performed to detect the indicated proteins.

(G) MKK4/7 DKO MEF were transfected with vector expressing Flag-MLK3 or its Y53A or P470A mutants and treated with SS and 5 mM TFMB-2-HG as in (C). IP, in vitro kinase assay, and WB were performed to detect the indicated proteins.

(H) HEK293T cells co-transfected with vectors expressing HA-Cdc42 and Flag-MLK3 or its mutants (as indicated) were treated with SS and 5 mM TFMB-2-HG for 9 hr, followed by IP and WB as in (A).

(I) WB to detect the indicated proteins in U87 MG cells that expressed control shRNA or shRNA against *Cdc42* and were subjected (+) or not (–) to SS for 9 hr.

(J) WB to detect Cdc42 in TCL of WT MEF that were incubated with the indicated doses of 2-HG for 1 hr on ice and another 0.5 hr at room temperature, followed by pronase digestion for 10 min.

SS remained intact and was still abrogated by 2-HG (Figure 5H). These results validate our hypothesis that SS-induced activation of MLK3 is due to Cdc42-mediated interference with MLK3's auto-inhibition. Because 2-HG disrupts the association of Cdc42 with MLK3, MLK3 is maintained in its auto-inhibited state and cannot activate downstream kinases, such as JNK. In agreement with this theory, knockdown of Cdc42 in U87 MG cells abolished SS-induced JNK activation in vitro (Figure 5I).

To investigate how 2-HG disrupts the interaction between Cdc42 and MLK3, we carried out drug affinity responsive target stability (DARTS) assays in vitro (Fu et al., 2015; Lomenick et al., 2009). These experiments showed that 2-HG could efficiently protect Cdc42 and TET2 (as a positive control) from digestion by pronase, implying the direct binding of 2-HG to Cdc42 (Figures 5J, S4A, and S4B). Moreover, the maximal fluorescence intensity of GST-Cdc42 and a well-known 2-HG-binding protein PHD2, but not GST, was quenched by 2-HG in a dose-dependent manner (Figures S4C and S4D). These data provide additional evidence that 2-HG can bind directly to Cdc42 and disrupt its interaction with MLK3.

SS-Induced Apoptosis Is Antagonized by Mutated IDH1

Because JNK activation plays a crucial role in SS-induced apoptosis and our data indicated that IDH1-R132H/Q mutations could dramatically block JNK activation, we examined whether this inhibition allowed a cell to escape SS-induced apoptosis. We exposed WT and IDH1-KI MEF to SS for 72 hr and assessed their viability by Annexin V staining and flow cytometry. We found that <45% of WT MEF survived this treatment, whereas IDH1-KI MEF had a survival rate of close to 80% (Figure 6A). Consistent with this result, overexpression of IDH1-R132H in U87 MG cells markedly suppressed SS-induced cell death, and inhibition of 2-HG production with AGI-5198 rendered U87 MG cells once again sensitive to SS (Figure 6B). Furthermore, 2-HG treatment reduced the sensitivity of WT MEF to SS-induced death, demonstrating that 2-HG plays a central role in the suppression of cell death mediated by mutated IDH1 (Figure 6C). Moreover, inhibition of JNK activity with the small molecule inhibitor SP600125 increased the resistance of WT MEF to SS-induced apoptosis (Figure 6D). Finally, overexpression of JNK-CA, a constitutively active form of JNK (Zheng et al., 1999), efficiently induced the apoptosis of WT MEF and IDH-KI MEF to the same extent, even without SS exposure (Figure 6E). Collectively, these data support our theory that IDH1 R132 mutations protect cells from SS-induced apoptosis by suppressing JNK activation.

To confirm our data showing that MLK3 and Cdc42 are required for SS-induced JNK activation and apoptosis (Figures 4B and 5I), we performed shRNA-mediated knockdown of either MLK3 or Cdc42 in U87 MG cells and observed a pronounced increase in cell survival in both cases (Figure 6F). Interestingly, expression of a constitutively active form of MLK3 (MLK3 Y53A) in WT and IDH1-KI MEF triggered robust apoptosis to the same extent (Figures 6G and 6H), consistent with our examination of MKK7 activation (Figure 5G). In contrast, overexpression of the inactive ΔCRIB MLK3 mutant failed to induce the death of WT or IDH1-KI MEF (Figures 6G and 6H). Taken together, these data establish that the SS-induced apoptosis mediated by JNK activation is antagonized by mutated IDH1 because of the effects of this abnormal enzyme on MLK3 and Cdc42.

Mutant IDH1 Inhibits SS-Induced Apoptosis by Diminishing Bim Phosphorylation

Caspase activation is a key event in apoptosis execution and is often used as an indicator of its occurrence. We observed that the cleavage of caspase3 in WT MEF cultures occurred much earlier and more intensely than in IDH1-KI MEF cultures (Figure S5A), consistent with the MEF survival rates shown in Figure 6A. It has been previously shown that JNK-mediated phosphorylation of the BH3-only protein Bim at Ser65 is required for neuronal apoptosis induced by survival factor withdrawal (Putcha et al., 2003). As expected, we found by western blotting that the phosphorylation of Bim was markedly higher in SS-treated WT MEF than in IDH1-KI MEF (Figure S5A). The inhibition of JNK activity by either SP600125 (Figure S5B) or 2-HG (Figure S5C) abrogated Bim phosphorylation in SS-treated WT MEF and blocked apoptosis, as indicated by caspase3 cleavage. Conversely, the restoration of JNK activity in IDH1-KI MEF by overexpression of JNK-CA significantly increased Bim phosphorylation and caspase3 cleavage (Figure S5D). Lastly, we treated U87 MG cells with SS plus 2-HG and found that JNK phosphorylation, Bim phosphorylation, and caspase3 cleavage were all inhibited in parallel (Figure S5E). These results indicate that under the conditions of serum deprivation, 2-HG suppresses Bim phosphorylation by inhibiting JNK signaling and thus protects cells from apoptotic death.

Tumorigenicity of IDH1-R132H/Q Mutant Enzymes Depends on JNK Inhibition

The above data clearly establish that IDH1-R132 mutation abrogates SS-induced apoptosis by suppressing JNK activation. Because apoptosis is a natural barrier to tumor progression, we suspected that the tumorigenicity of the IDH1-R132H/Q mutant enzymes might be due to their inhibition of JNK. To test this possibility, we examined the relationship between JNK activity and IDH1 mutation in clinical specimens from patients with low-grade glioma. JNK activity and caspase-3 cleavage in glioma samples with IDH1-R132H mutation was markedly lower than in glioma samples expressing WT IDH1/2 (Figures 7A and S6), in line with our theory that inhibition of JNK-mediated apoptosis may be involved in the development of tumors driven by mutant IDH1. We next used cBioPortal (Cerami et al., 2012) to analyze phosphorylation levels of c-Jun, a JNK substrate, in lower grade gliomas chosen from 268 patients annotated in The Cancer Genome Atlas (TCGA) database. We found that gliomas bearing an IDH1 R132 mutation (211 patients) had much lower pS73-c-Jun levels than gliomas expressing WT IDH1 (57 patients) (Figure S7A).

To confirm this observation in a living animal, we performed tumor allograft assays, in which nude mice were injected with 2×10^6 WT MEF in the left flank and 2×10^6 IDH1-KI MEF in the right flank and tumor growth was determined at 3 weeks post-injection. As expected, IDH1-KI MEF displayed much more potency in tumor formation than did WT MEF (Figure 7B, left and middle panel), and JNK activity (Figure 7B, right panel) and apoptotic rate (Figure S7B) in allograft tumors derived from IDH1-KI MEF was dramatically suppressed, whereas proliferation rate, as monitored by PCNA expression (Figure S7B), was not influenced by the IDH1 R132Q mutant. Consistent with these results, the tumorigenicity of IDH1-KI MEF was diminished by overexpression of JNK-CA (Figure 7C). These results provide convincing evidence that the tumor-promoting ability of the IDH1-R132 mutant enzymes depends, at least in part, on their inhibitory effects on JNK-mediated apoptosis.

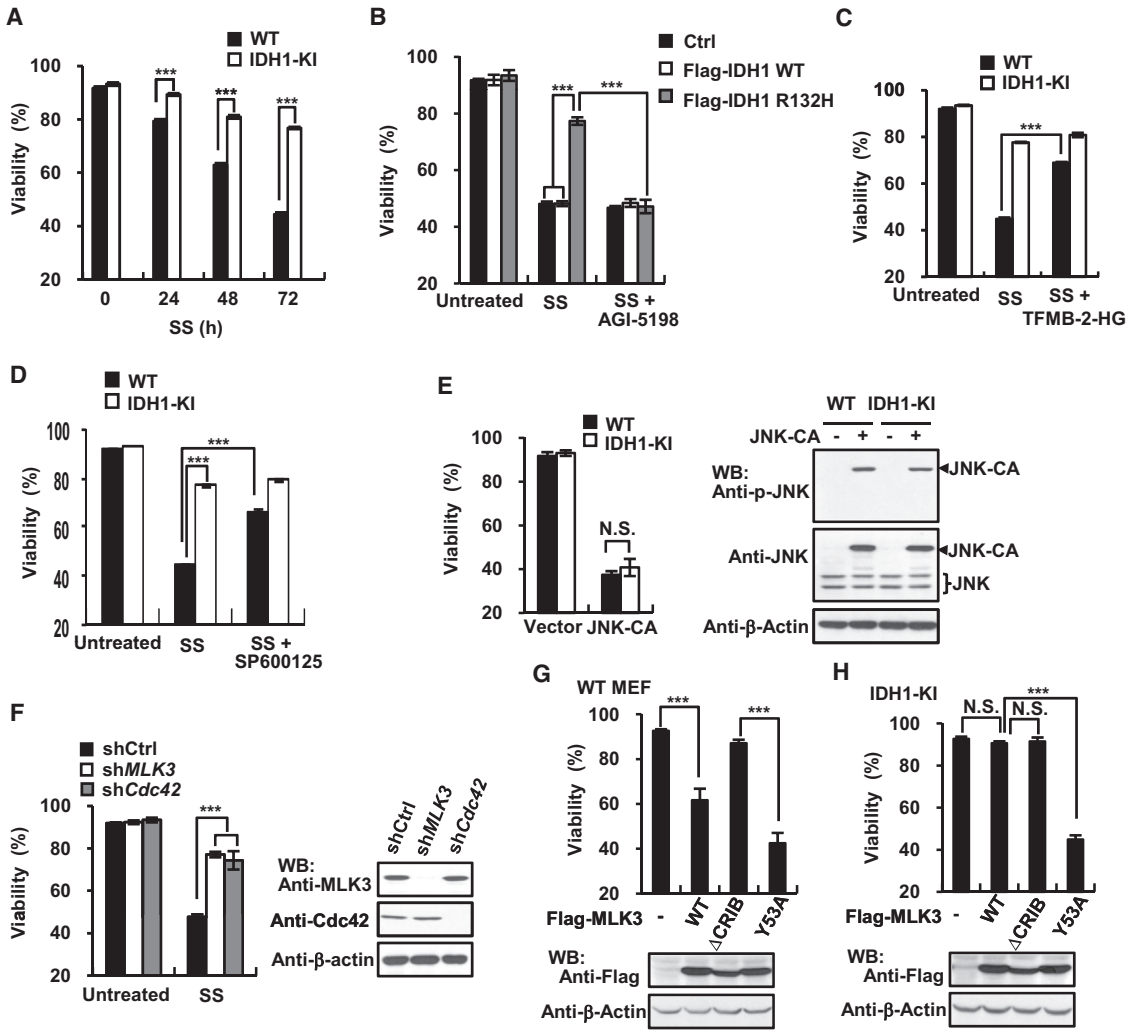

Figure 6. SS-induced Cell Death Is Mediated by JNK and Antagonized by IDH1 Mutation

(A) Viability as determined by FITC-Annexin V staining and flow cytometry of WT MEF and IDH1-KI MEF that were subjected to SS for the indicated times. Data are the mean ± SD of three independent experiments. ***$p < 0.001$, unpaired Student's t test. N.S., not significant.

(B) Viability determined as in (A) of U87 MG cells expressing control vector (Ctrl) or Flag-tagged WT IDH1 or IDH1-R132H, which were left untreated, deprived of serum for 72 hr, or pretreated with 1.5 μM AGI-5198 for 2 days, followed by serum deprivation for 72 hr in the presence of AGI-5198.

(C) Viability determined as in (A) of WT MEF and IDH1-KI MEF that were left untreated, deprived of serum for 72 hr, or exposed to 5 mM TFMB-2-HG during SS for 72 hr.

(D) Viability determined as in (A) of WT MEF and IDH1-KI MEF that were left untreated, deprived of serum for 72 hr, or exposed to SP600125 (10 μM) during SS for 72 hr.

(E) Left: viability determined as in (A) of WT MEF and IDH1-KI MEF transfected with empty vector or vector expressing JNK-CA. Right: WB to detect the indicated proteins in TCL of the cells in the left panel.

(F) Left: viability determined as in (A) of U87 MG cells expressing control shRNA (shCtrl) or shRNA against *MLK3* or *Cdc42*, which were left untreated or deprived of serum for 72 hr. Right: WB to detect the indicated proteins in TCL of the cells in the left panel.

(G and H) WT MEF (G) and IDH1-KI MEF (H) were transfected with vector expressing Flag-WT MLK3, MLK3-ΔCRIB, or MLK3-Y53A. Viability (top panels) and WB to detect the indicated proteins (bottom panels) were determined as in (E).

In conclusion, our study demonstrates that the high level of 2-HG produced by cancer-associated IDH mutations endows cells with the ability to resist death induced by nutrient deprivation, a scenario frequently encountered in a rapidly growing tumor mass. We have further shown that this resistance is due to disruption of the Cdc42-MLK3-MKK4/7-JNK-Bim pro-apoptotic cascade. We propose that these effects play a critical role in the tumorigenesis driven by IDH mutations (Figure 7D).

DISCUSSION

Precisely how IDH1/2 mutations promote tumorigenesis has been widely investigated in recent years. It is clear that 2-HG, the product of the abnormal reaction mediated by these mutant enzymes, has important effects, such as the promotion of DNA and histone methylation, enhancement of HIF-1α stability, and dysregulation of cellular redox status (Lu et al., 2012; Noushmehr

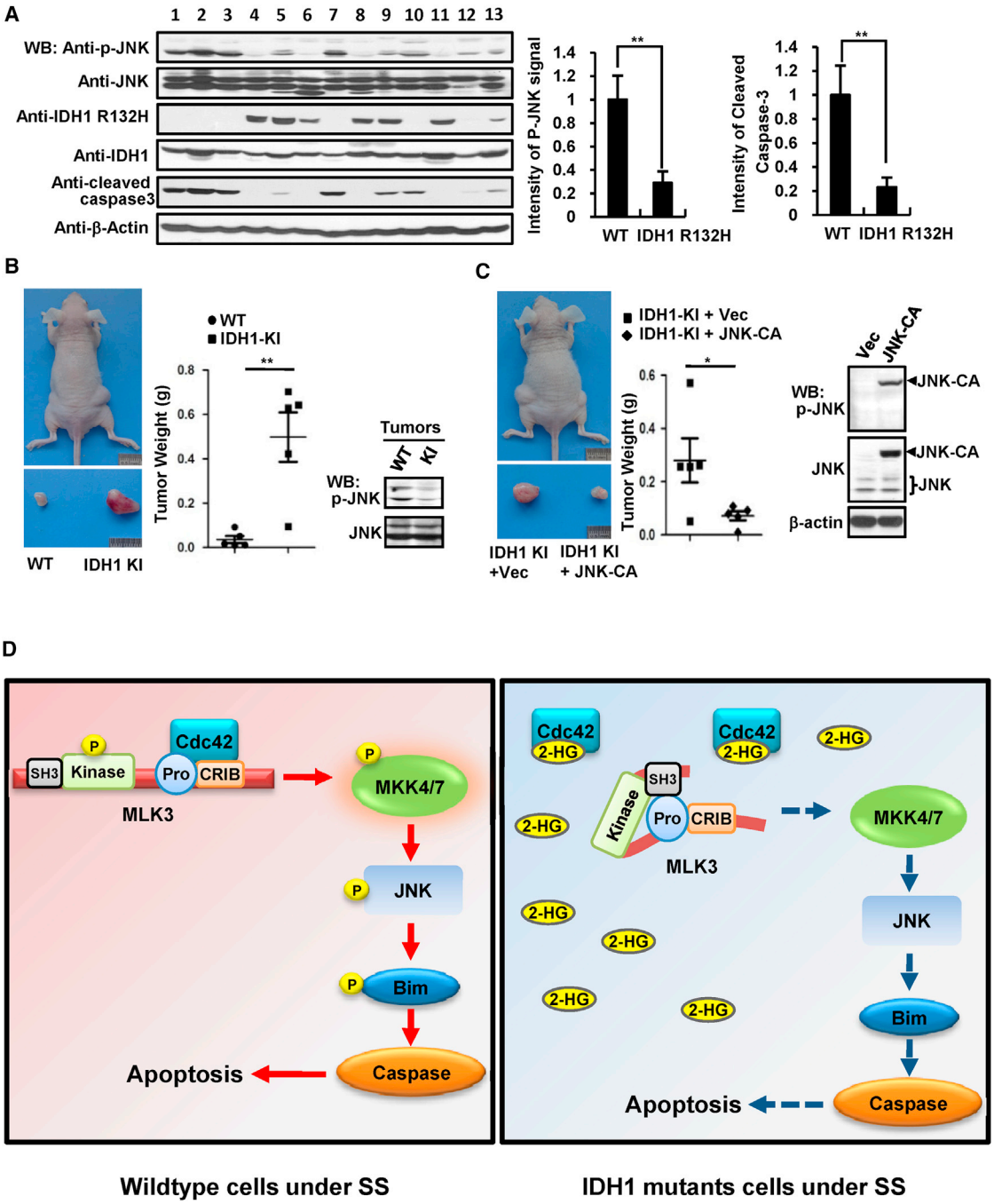

Figure 7. Tumor-Promoting Ability of the IDH1-R132 Mutant Enzyme Depends on Its Inhibitory Effect on JNK

(A) WB to detect the indicated proteins in clinical human glioma samples, some of which have WT IDH1 and some of which have an IDH1-R132H mutation (left). Quantitation of signal intensities of WB bands of p-JNK (middle) and Cleaved caspase3 (right) using ImageJ software. p-JNK levels were normalized to total JNK levels and cleaved caspase-3 were normalized to β-actin levels, respectively. Data were grouped by WT or mutant IDH1 expression and are presented as the mean ± SEM (**$p < 0.01$, unpaired Student's t test).

(B) Primary IDH1 WT and IDH1-KI MEF were injected subcutaneously into contralateral flanks of nude mice (n = 5) and allograft tumors were allowed to form (see Supplemental Experimental Procedures). Mice were sacrificed at 3 weeks post-injection. Left: gross appearance of a representative allograft tumor-bearing mouse, and representative tumors isolated from IDH1 WT and IDH1-KI allograft-bearing mice. Middle: quantitation of tumor weights. Dots represent weights of individual tumors in n = 5 mice/group. The mean ± SEM are also indicated (**$p < 0.01$, unpaired Student's t test). Right: WB to detect the indicated proteins in IDH1 WT and IDH1-KI allograft tumors.

(C) IDH1-KI MEF were infected with empty lentivirus (Vec) or lentivirus expressing JNK-CA (n = 5/group) and allograft tumor assays were performed and analyzed as in (B).

(legend continued on next page)

et al., 2010; Sasaki et al., 2012b; Turcan et al., 2012; Xu et al., 2011; Zhao et al., 2009). All these aspects converge at the molecular level on dioxygenases that use α-KG as a substrate, so are inhibited by the high levels of 2-HG present in cells expressing IDH1/2 mutant enzymes. However, there has been little investigation into the regulatory effects of 2-HG on enzymes other than dioxygenases. A previous study revealed that 2-HG can directly bind to and suppress ATP synthase (Fu et al., 2015), suggesting that the identification of 2-HG-binding proteins other than dioxygenases may be important to clarify how 2-HG promotes tumorigenesis. Given that 2-HG can reach concentrations as high as 5–35 mM in clinical samples harboring IDH1/2 mutations (Dang et al., 2009), the matter may be vitally important to resolve.

Our study has shown that Cdc42, a Rho family GTPase and also an activator of MLK3 in response to SS, is a 2-HG binding protein. In cells harboring mutated IDH1, 2-HG binding prevents Cdc42's association with MLK3. As a result, activation of the MLK3-MKK4/7-JNK cascade is abolished in IDH1-mutated cells because the unfolding of the MLK3 intramolecular loop induced by Cdc42 interaction is a prerequisite for SS-triggered MLK3 activation. To determine if the concentration of endogenous 2-HG in IDH1 mutant cells was sufficient to interact with Cdc42 and block its association with MLK3, we used an intrinsic fluorescence assay to measure the dissociation constant (K_d) of exogenous 2-HG complexed with Cdc42. We found that 2-HG has a K_d of 211.61 ± 16.99 μM, which is much lower than the millimolar 2-HG concentrations present in IDH1/2 mutant cells (Dang et al., 2009). This result implies that the majority of Cdc42 molecules in IDH1/2 mutant cells may be bound to 2-HG, consistent with the result of our DARTS assays showing that a 400 μM concentration of 2-HG can protect Cdc42 from pronase digestion.

Cancer is a disease of dysregulation of not only cellular proliferation and differentiation, but also apoptosis. Various types of programmed cell death are triggered by particular physiological stresses in specific contexts, and those mechanisms serve as important natural barriers to cancer initiation and development. Accordingly, a deficiency or inhibition of programmed cell death often leads to tumorigenesis. Unlike normal cells, tumor cells in rapidly expanding cancers are frequently exposed to hypoxia and inadequate supplies of nutrients and growth factors. This scenario is exacerbated in a solid tumor microenvironment because these masses often have an inefficient or insufficient vasculature and so a limited blood supply. Mammalian cells have evolved various cellular processes, including autophagy and apoptosis, to deal with nutrient starvation. Sublethal levels of nutrient deficiency generally trigger autophagy, which provides a cell with a basic level of nutrients through digestion of organelles and proteins unnecessary for maintaining survival (Klionsky and Emr, 2000). However, severe nutrient deficiency (as occurs in SS) eventually induces apoptosis. In the context of cancer, this apoptosis acts as a mechanism to eliminate rapidly proliferating tumor cells and limit the expanding cancerous mass (Izuishi et al., 2000; Ou et al., 2006). Although some cancer cells become tolerant to SS due to the acquisition of mutations that drive excessive or constitutive activation of the PI3K/AKT pathway (Izuishi et al., 2000), apoptosis may still play a key role in preventing tumorigenesis at its very early stages before incipient tumor cells acquire resistance to death induced by nutrient deprivation. Relevant to our study, a well-characterized apoptotic pathway triggered by SS or survival factor withdrawal involves JNK activation and subsequent Bim phosphorylation (Putcha et al., 2003).

We found out that SS induced JNK activation, and apoptosis was dramatically inhibited by the high levels of 2-HG produced by the IDH1-R132Q mutant enzyme. At the mechanistic level, we established that 2-HG can bind directly to Cdc42 and block its interaction with MLK3, thus switching off the Cdc42-MLK3-MKK4/7-JNK cascade induced by SS. Nevertheless, two important questions remain. First, how is Cdc42 activated to associate with MLK3 in response to SS? To answer this question, we need to identify the possible covalent modifications and binding partners of Cdc42 that facilitate its interaction with MLK3. Second, why is 2-HG-bound Cdc42 unable to interact with MLK3? One possibility is that 2-HG induces a significant conformational change in the Cdc42 protein structure that disrupts the interface used for association with MLK3. Structural biology studies are now under way, with the goal of defining the co-crystal structure of 2-HG and Cdc42.

In conclusion, our study has revealed that 2-HG-mediated inhibition of SS-induced, JNK-mediated apoptosis may be a key event in the tumorigenesis promoted by IDH1/2 mutations. Such a mechanism represents an important complement to the diverse aspects already pinpointed as underlying the initiation and progression of various cancers harboring 2-HG-producing IDH1/2 mutant enzymes. Noteworthily, the loss of expression of the JNK3 gene in 10 of the 19 human brain-tumor cell lines was found in the previous study (Yoshida et al., 2001), but most of these cell lines are not IDH1 mutant cell lines. This might raise an issue that IDH1/2 mutations are not the only mechanism to block the JNK-mediated apoptosis in gliomas. JNK deficiency caused by other mechanisms, such as allelic loss and promoter methylation, may also lead to brain tumorigenesis.

EXPERIMENTAL PROCEDURES

Cell Lines, Reagents, Antibodies, and Constructs

Detailed information on cell lines, reagents, antibodies, and constructs is described in the Supplemental Experimental Procedures.

In Vitro MLK3 Kinase Assay

Flag-tagged WT MLK3 or mutant MLK3, in which the CRIB motif was deleted (MLK3ΔCRIB), was immunoprecipitated from untreated or SS-treated

(D) A model proposing how SS-stimulated JNK-mediated apoptosis is inhibited by 2-HG in cells expressing mutated IDH1. Left: in WT cells deprived of nutrients, Cdc42 associates with MLK3 at its CRIB motif, inducing successive phosphorylation of MKK4/7, JNK, and Bim. Caspase-mediated apoptosis is thus triggered, killing any incipient tumor cell. Right: in cells expressing mutated IDH1 and deprived of nutrients, the high levels of 2-HG produced by the mutant enzyme bind to Cdc42 and prevent it from complexing to MLK3 at the CRIB motif. MLK3 is thus not activated even under conditions of nutrient insufficiency. As a result, the MKK4/7-JNK-Bim cascade is not triggered, allowing the mutated cell to survive. This incipient tumor cell may then acquire additional oncogenic mutations that cause it to transform and become malignant.

MKK4/7 DKO MEF using anti-Flag M2 beads (Sigma). Immunoprecipitates were washed three times in lysis buffer, twice in kinase buffer (10 mM HEPES [pH = 7.4], 1 mM DTT, 5 mM $MgCl_2$, and 1 mM ATP), and incubated with 2 μg of purified His-tagged MKK4 or MKK7 for 30 min at 37°C. Reactions were stopped by the addition of gel-loading buffer and subjected to SDS-PAGE to fractionate proteins, followed by WB with the appropriate antibodies.

Flow Cytometric Cell Death Assay

Cells cultured in six-well plates were left untreated or subjected to serum withdrawal for the times indicated in the Figures. After treatment, suspended and trypsinized cells were centrifuged at 800 × *g* for 5 min, washed once with PBS, and stained with FITC-conjugated Annexin V for 10 min at 37°C in the dark. Percentages of apoptotic cells were quantified by sorting fluorescence-activated cell sorting using a flow cytometer.

DARTS Assay

DARTS assays were performed as described (Lomenick et al., 2009), with some modifications. For detailed information, please refer to the Supplemental Experimental Procedures.

LC-MS

2-HG levels were determined by LC-MS as described previously (Dang et al., 2009). For detailed information, please refer to the Supplemental Experimental Procedures.

Animal Experiments and Patient Samples

All animal experimental protocols were approved by the institutional Animal Care and Use Committee at Xiamen University. Glioma samples were obtained with the approval of the research ethics boards of Xiamen University and Huanhu Hospital. Written informed consent was obtained from all patients. For detailed information, please refer to the Supplemental Experimental Procedures.

Data Analysis

The two-tailed Student's t test was used to compare differences between treated groups and their controls. Differences were considered significant if p values were lower than 0.05; *$p < 0.05$; **$p < 0.01$; ***$p < 0.001$.

SUPPLEMENTAL INFORMATION

Supplemental Information includes Supplemental Experimental Procedures and seven figures and can be found with this article online at http://dx.doi.org/10.1016/j.celrep.2017.03.053.

AUTHOR CONTRIBUTIONS

B.J., J.Z., J.X., and Q.L. conceived the project. B.J. and Q.L. designed most of the experiments. B.J., J.Z., J.X., W.Z., Y.W., A.C., H.M., Q.Z., M.S., F.L., L.Z., J.W., and Y.Z. performed experiments and discussed results. M.S., L.L., H.Z., Y.H., X.L., L.-M.H., T.W.M., and Q.L. discussed and interpreted the data. B.J., J.Z., and Q.L. wrote the original manuscript, and L.-M.H., T.W.M., and Q.L. refined the paper.

ACKNOWLEDGMENTS

This work was supported by the National Natural Science Foundation of China (81372702, 81402285, and 31571473), the Fundamental Research Funds for the Central Universities (20720140552 and 10120100002), the Specialized Research Fund for the Doctoral Program of Higher Education of China (20120121110005), the National Science Foundation of China for Fostering Talents in Basic Research (grant no. J1310027), and the 111 Project of Education of China (B06016). We thank Dr. Sheng-Cai Lin for kindly providing pCMV5-Flag-JNK1, pGEX-4T-1-MKK4/7, and pGL3-fos-7LEF-luciferase plasmids. We are grateful to Dr. M. Saunders for scientific editing of the manuscript.

Received: December 13, 2016
Revised: February 16, 2017
Accepted: March 17, 2017
Published: April 11, 2017

REFERENCES

Amary, M.F., Bacsi, K., Maggiani, F., Damato, S., Halai, D., Berisha, F., Pollock, R., O'Donnell, P., Grigoriadis, A., Diss, T., et al. (2011). IDH1 and IDH2 mutations are frequent events in central chondrosarcoma and central and periosteal chondromas but not in other mesenchymal tumours. J. Pathol. *224*, 334–343.

Böck, B.C., Vacratsis, P.O., Qamirani, E., and Gallo, K.A. (2000). Cdc42-induced activation of the mixed-lineage kinase SPRK in vivo. Requirement of the Cdc42/Rac interactive binding motif and changes in phosphorylation. J. Biol. Chem. *275*, 14231–14241.

Burbelo, P.D., Drechsel, D., and Hall, A. (1995). A conserved binding motif defines numerous candidate target proteins for both Cdc42 and Rac GTPases. J. Biol. Chem. *270*, 29071–29074.

Cerami, E., Gao, J., Dogrusoz, U., Gross, B.E., Sumer, S.O., Aksoy, B.A., Jacobsen, A., Byrne, C.J., Heuer, M.L., Larsson, E., et al. (2012). The cBio cancer genomics portal: an open platform for exploring multidimensional cancer genomics data. Cancer Discov. *2*, 401–404.

Coso, O.A., Chiariello, M., Yu, J.C., Teramoto, H., Crespo, P., Xu, N., Miki, T., and Gutkind, J.S. (1995). The small GTP-binding proteins Rac1 and Cdc42 regulate the activity of the JNK/SAPK signaling pathway. Cell *81*, 1137–1146.

Dang, L., White, D.W., Gross, S., Bennett, B.D., Bittinger, M.A., Driggers, E.M., Fantin, V.R., Jang, H.G., Jin, S., Keenan, M.C., et al. (2009). Cancer-associated IDH1 mutations produce 2-hydroxyglutarate. Nature *462*, 739–744.

Figueroa, M.E., Abdel-Wahab, O., Lu, C., Ward, P.S., Patel, J., Shih, A., Li, Y., Bhagwat, N., Vasanthakumar, A., Fernandez, H.F., et al. (2010). Leukemic IDH1 and IDH2 mutations result in a hypermethylation phenotype, disrupt TET2 function, and impair hematopoietic differentiation. Cancer Cell *18*, 553–567.

Fu, X., Chin, R.M., Vergnes, L., Hwang, H., Deng, G., Xing, Y., Pai, M.Y., Li, S., Ta, L., Fazlollahi, F., et al. (2015). 2-Hydroxyglutarate inhibits ATP synthase and mTOR signaling. Cell Metab. *22*, 508–515.

Garrington, T.P., and Johnson, G.L. (1999). Organization and regulation of mitogen-activated protein kinase signaling pathways. Curr. Opin. Cell Biol. *11*, 211–218.

Harris, C.A., Deshmukh, M., Tsui-Pierchala, B., Maroney, A.C., and Johnson, E.M., Jr. (2002). Inhibition of the c-Jun N-terminal kinase signaling pathway by the mixed lineage kinase inhibitor CEP-1347 (KT7515) preserves metabolism and growth of trophic factor-deprived neurons. J. Neurosci. *22*, 103–113.

Hirata, M., Sasaki, M., Cairns, R.A., Inoue, S., Puviindran, V., Li, W.Y., Snow, B.E., Jones, L.D., Wei, Q., Sato, S., et al. (2015). Mutant IDH is sufficient to initiate enchondromatosis in mice. Proc. Natl. Acad. Sci. USA *112*, 2829–2834.

Inoue, S., Li, W.Y., Tseng, A., Beerman, I., Elia, A.J., Bendall, S.C., Lemonnier, F., Kron, K.J., Cescon, D.W., Hao, Z., et al. (2016). Mutant IDH1 downregulates ATM and alters DNA repair and sensitivity to DNA damage independent of TET2. Cancer Cell *30*, 337–348.

Izuishi, K., Kato, K., Ogura, T., Kinoshita, T., and Esumi, H. (2000). Remarkable tolerance of tumor cells to nutrient deprivation: possible new biochemical target for cancer therapy. Cancer Res. *60*, 6201–6207.

Klionsky, D.J., and Emr, S.D. (2000). Autophagy as a regulated pathway of cellular degradation. Science *290*, 1717–1721.

Koivunen, P., Lee, S., Duncan, C.G., Lopez, G., Lu, G., Ramkissoon, S., Losman, J.A., Joensuu, P., Bergmann, U., Gross, S., et al. (2012). Transformation by the (R)-enantiomer of 2-hydroxyglutarate linked to EGLN activation. Nature *483*, 484–488.

Liu, Y.F., Dorow, D., and Marshall, J. (2000). Activation of MLK2-mediated signaling cascades by polyglutamine-expanded huntingtin. J. Biol. Chem. *275*, 19035–19040.

Lomenick, B., Hao, R., Jonai, N., Chin, R.M., Aghajan, M., Warburton, S., Wang, J., Wu, R.P., Gomez, F., Loo, J.A., et al. (2009). Target identification using drug affinity responsive target stability (DARTS). Proc. Natl. Acad. Sci. USA *106*, 21984–21989.

Lu, C., Ward, P.S., Kapoor, G.S., Rohle, D., Turcan, S., Abdel-Wahab, O., Edwards, C.R., Khanin, R., Figueroa, M.E., Melnick, A., et al. (2012). IDH mutation impairs histone demethylation and results in a block to cell differentiation. Nature *483*, 474–478.

Mardis, E.R., Ding, L., Dooling, D.J., Larson, D.E., McLellan, M.D., Chen, K., Koboldt, D.C., Fulton, R.S., Delehaunty, K.D., McGrath, S.D., et al. (2009). Recurring mutations found by sequencing an acute myeloid leukemia genome. N. Engl. J. Med. *361*, 1058–1066.

Minden, A., Lin, A., Claret, F.X., Abo, A., and Karin, M. (1995). Selective activation of the JNK signaling cascade and c-Jun transcriptional activity by the small GTPases Rac and Cdc42Hs. Cell *81*, 1147–1157.

Noushmehr, H., Weisenberger, D.J., Diefes, K., Phillips, H.S., Pujara, K., Berman, B.P., Pan, F., Pelloski, C.E., Sulman, E.P., Bhat, K.P., et al.; Cancer Genome Atlas Research Network (2010). Identification of a CpG island methylator phenotype that defines a distinct subgroup of glioma. Cancer Cell *17*, 510–522.

Ou, X.M., Chen, K., and Shih, J.C. (2006). Monoamine oxidase A and repressor R1 are involved in apoptotic signaling pathway. Proc. Natl. Acad. Sci. USA *103*, 10923–10928.

Parsons, D.W., Jones, S., Zhang, X., Lin, J.C., Leary, R.J., Angenendt, P., Mankoo, P., Carter, H., Siu, I.M., Gallia, G.L., et al. (2008). An integrated genomic analysis of human glioblastoma multiforme. Science *321*, 1807–1812.

Putcha, G.V., Le, S., Frank, S., Besirli, C.G., Clark, K., Chu, B., Alix, S., Youle, R.J., LaMarche, A., Maroney, A.C., et al. (2003). JNK-mediated BIM phosphorylation potentiates BAX-dependent apoptosis. Neuron *38*, 899–914.

Rohle, D., Popovici-Muller, J., Palaskas, N., Turcan, S., Grommes, C., Campos, C., Tsoi, J., Clark, O., Oldrini, B., Komisopoulou, E., et al. (2013). An inhibitor of mutant IDH1 delays growth and promotes differentiation of glioma cells. Science *340*, 626–630.

Sasaki, M., Knobbe, C.B., Itsumi, M., Elia, A.J., Harris, I.S., Chio, I.I., Cairns, R.A., McCracken, S., Wakeham, A., Haight, J., et al. (2012a). D-2-hydroxyglutarate produced by mutant IDH1 perturbs collagen maturation and basement membrane function. Genes Dev. *26*, 2038–2049.

Sasaki, M., Knobbe, C.B., Munger, J.C., Lind, E.F., Brenner, D., Brüstle, A., Harris, I.S., Holmes, R., Wakeham, A., Haight, J., et al. (2012b). IDH1(R132H) mutation increases murine haematopoietic progenitors and alters epigenetics. Nature *488*, 656–659.

Teramoto, H., Coso, O.A., Miyata, H., Igishi, T., Miki, T., and Gutkind, J.S. (1996). Signaling from the small GTP-binding proteins Rac1 and Cdc42 to the c-Jun N-terminal kinase/stress-activated protein kinase pathway. A role for mixed lineage kinase 3/protein-tyrosine kinase 1, a novel member of the mixed lineage kinase family. J. Biol. Chem. *271*, 27225–27228.

Turcan, S., Rohle, D., Goenka, A., Walsh, L.A., Fang, F., Yilmaz, E., Campos, C., Fabius, A.W., Lu, C., Ward, P.S., et al. (2012). IDH1 mutation is sufficient to establish the glioma hypermethylator phenotype. Nature *483*, 479–483.

Ward, P.S., Patel, J., Wise, D.R., Abdel-Wahab, O., Bennett, B.D., Coller, H.A., Cross, J.R., Fantin, V.R., Hedvat, C.V., Perl, A.E., et al. (2010). The common feature of leukemia-associated IDH1 and IDH2 mutations is a neomorphic enzyme activity converting alpha-ketoglutarate to 2-hydroxyglutarate. Cancer Cell *17*, 225–234.

Xu, Z., Maroney, A.C., Dobrzanski, P., Kukekov, N.V., and Greene, L.A. (2001). The MLK family mediates c-Jun N-terminal kinase activation in neuronal apoptosis. Mol. Cell. Biol. *21*, 4713–4724.

Xu, W., Yang, H., Liu, Y., Yang, Y., Wang, P., Kim, S.H., Ito, S., Yang, C., Wang, P., Xiao, M.T., et al. (2011). Oncometabolite 2-hydroxyglutarate is a competitive inhibitor of α-ketoglutarate-dependent dioxygenases. Cancer Cell *19*, 17–30.

Yan, H., Parsons, D.W., Jin, G., McLendon, R., Rasheed, B.A., Yuan, W., Kos, I., Batinic-Haberle, I., Jones, S., Riggins, G.J., et al. (2009). IDH1 and IDH2 mutations in gliomas. N. Engl. J. Med. *360*, 765–773.

Yoshida, S., Fukino, K., Harada, H., Nagai, H., Imoto, I., Inazawa, J., Takahashi, H., Teramoto, A., and Emi, M. (2001). The c-Jun NH2-terminal kinase3 (JNK3) gene: genomic structure, chromosomal assignment, and loss of expression in brain tumors. J. Hum. Genet. *46*, 182–187.

Zhang, H., and Gallo, K.A. (2001). Autoinhibition of mixed lineage kinase 3 through its Src homology 3 domain. J. Biol. Chem. *276*, 45598–45603.

Zhao, S., Lin, Y., Xu, W., Jiang, W., Zha, Z., Wang, P., Yu, W., Li, Z., Gong, L., Peng, Y., et al. (2009). Glioma-derived mutations in IDH1 dominantly inhibit IDH1 catalytic activity and induce HIF-1alpha. Science *324*, 261–265.

Zheng, C., Xiang, J., Hunter, T., and Lin, A. (1999). The JNKK2-JNK1 fusion protein acts as a constitutively active c-Jun kinase that stimulates c-Jun transcription activity. J. Biol. Chem. *274*, 28966–28971.